Electronic Supplementary Information

for

Revisiting Zinc Coordination in Human Carbonic Anhydrase II

He Song, David L. Wilson, Erik R. Farquhar, Edwin A. Lewis, and Joseph P. Emerson

Contents:

Table S1. Summarized stability constants and formation enthalpies for Zn^{2+}-Buffer and H^{+}-Buffer [a]

Buffer	$\log K_{H\text{-}Buff}$	$\Delta H_{H\text{-}Buff}$ (kcal/mol)	$\log K_{1,ZnBuff}$	$\log \beta_{2,Zn\text{-}Buff}$	$\Delta H_{Zn\text{-}Buff}$ (kcal/mol)
PIPES	6.93	-2.78	3.07		0.46
MOPS	7.18	-5.01	3.22		-0.09[b]
ACES	6.79	-9.34	2.34	3.74	-5.18
Tris	8.10	-11.36	2.27		-2.02

[a] from ref S1. Values are determined under conditions of 25°C, μ=0.1, pH 7.4, and 100 mM concentration. [b] from ref S2.

Table S2 . Thermodynamic cycle for Zn^{2+} binding to apoCA in 100 mM ACES, pH = 7.4

eq	reaction	coeff	ΔH° (kcal/mol)	ΔG° (kcal/mol)
	0.33 $Zn(ACES)^{2+}$ + 0.66 $Zn(ACES)_2^{2+}$ + $(H^+)_{0.9}$-CA → $ZnCA^{2+}$ + 0.9 H^+ACES + 0.75 ACES		-7.4[a]	-8.2[a]
1	$Zn(ACES)^{2+}$ → Zn^{2+} + ACES	0.33	3.14[b]	3.19[b]
2	$Zn(ACES)_2^{2+}$ → Zn^{2+} + 2ACES	0.66	6.28[b]	5.10[b]
3	H^+-CA → H^+ + CA [c]	0.9	13.50[d]	9.27[e]
4	ACES + H^+ → H^+ACES	0.9	-9.34[b]	-9.26[b]
5	Zn^{2+} + CA → $ZnCA^{2+}$	1	-16.4	-12.6

[a] From Table 1. [b] From Table S1. [c] The reaction actually written as: $(His)_3Zn\text{-}H_2O$ → $(His)_3Zn\text{-}OH^-$ + H^+, explanation see text. [d] ref S3. [e] pK_a of zinc bound water is 6.8, ref S4. $\Delta G° = -RT\ln(K_a)$

Table S3 . Thermodynamic cycle for Zn^{2+} binding to apoCA in 100 mM MOPS, pH = 7.4

eq	reaction	coeff	ΔH° (kcal/mol)	ΔG° (kcal/mol)
	$Zn(MOPS)^{2+}$ + $(H^+)_{0.9}$-CA → $ZnCA^{2+}$ + 0.9 H^+MOPS + 0.1 MOPS		-8.1[a]	-8.6[a]
1	$Zn(MOPS)^{2+}$ → Zn^{2+} + MOPS	1	0.09[b]	4.39[b]
2	H^+-CA → H^+ + CA [c]	0.9	13.50[d]	9.27[e]
3	MOPS + H^+ → H^+MOPS	0.9	-5.01[b]	-9.79[b]
4	Zn^{2+} + CA → $ZnCA^{2+}$	1	-15.8	-12.6

[a] From Table 1. [b] From Table S1. [c] The reaction actually written as: $(His)_3Zn\text{-}H_2O$ → $(His)_3Zn\text{-}OH^-$ + H^+, explanation see text. [d] ref S3. [e] pK_a of zinc bound water is 6.8, ref S4. $\Delta G° = -RT\ln(K_a)$

Table S4. Fourier-filtered first-shell EXAFS analyses of as-isolated and reconstituted ZnCA.[a]

		Zn-N/O/(S)					
Sample	**fit**	**n**	**r**	**σ^2**	**F'**	**ΔE_0**	**BVS [b]**
As isolated (A)	1	3N	1.98	2.0	383	-5.52	1.58
	2	***4N***	***1.98***	***3.5***	***116***	***-5.79***	***2.10***
	3	5N	1.98	4.9	86	-6.45	2.65
	4	6N	1.97	6.2	165	-7.12	3.20
	5	3O	1.96	3.0	89	-3.69	1.66
	6	4O	1.96	4.8	55	-4.28	2.23
	7	5O	1.95	6.6	183	-5.05	2.80
	8	6O	1.95	8.5	594	-5.84	3.40
	9	*3N* *1O*	*2.01* *1.88*	*1.0* *-0.5*	*37*	*-5.93*	*2.21*
	10	4N 1O	1.99 1.87	3.6 4.0	74	-7.44	2.88
	11	2N 2O	2.03 1.91	0.2 1.5	23	-5.93	2.16
	12	3S	2.07	6.6	46	-27.99	-
	13	4S	2.07	8.7	52	-27.92	-
Reconstituted (B)	1	3N	1.98	1.8	253	-5.19	1.57
	2	***4N***	***1.98***	***3.3***	***88***	***-5.84***	***2.10***
	3	5N	1.98	4.7	100	-6.52	2.64
	4	6N	1.97	6.1	238	-7.31	3.20
	5	3O	1.96	2.9	53	-3.60	1.66
	6	4O	1.96	4.7	66	-4.39	2.23
	7	5O	1.95	6.5	283	-5.17	2.80
	8	6O	1.95	8.4	883	-5.98	3.40
	9	*3N* *1O*	*2.01* *1.90*	*2.0* *0.8*	*42*	*-5.72*	*2.21*
	10	4N 1O	1.97 1.84	3.3 12.4	89	-8.64	3.04
	11	2N 2O	2.02 1.92	1.4 2.6	31	-5.78	2.16
	12	3S	2.07	6.5	59	-28.81	-
	13	4S	2.07	8.7	119	-28.06	-

[a] r is in units of Å; σ^2 is in units of 10^{-3} Å^2; ΔE_0 is in units of eV. All fits are to Fourier-filtered EXAFS data, as follows: as-isolated ZnCA, k = 1.5 – 13.0 Å^{-1} (back transformation range = 0.6 – 2.1 Å, resolution = 0.14 Å); reconstituted ZnCA, k = 1.5 – 13.0 Å^{-1} (back transformation range = 0.6 – 2.1 Å, resolution = 0.14 Å).

[b] BVS = bond valence sum for the first-shell atoms of the fit. The BVS is defined as $\Sigma(\exp[(r_0 - r)/0.37])$, where r_0 is an empirically derived parameter for a given pair of atoms and r is the actual bond length. The average (1.74 Å) of the published r_0 values for Zn^{2+}–N and Zn^{2+}–O was used in the calculations. EXAFS cannot distinguish between atoms differing by Z ± 1.

Table S5. Selected unfiltered EXAFS fits to as-isolated ZnCA.[a]

	Zn-N/O			Zn•••C(His)					
fit	**n**	**r**	**σ^2**	**n**	**r**	**σ^2**	**F**	**F-factor**	**ΔE_0**
1	4	1.98	3.4				310	0.492	-5.73
2	5	1.97	4.8				307	0.490	-6.42
3	3 1	2.00 1.93	3.4 3.1				290	0.476	-5.37
4	4	1.98	3.3	6C	2.99	6.5	224	0.418	-6.34
5	***4***	***1.97***	***3.4***	***3His***	***2.99*** ***4.19*** ***4.21***	***6.5*** ***5.7*** ***5.7***	***127***	***0.314***	***-6.56***
6	4	1.97	3.3	4His	2.98 4.18 4.21	8.8 7.8 7.8	134	0.323	-6.96
7	4	1.97	3.4	2His	2.99 4.19 4.21	4.1 3.3 3.3	137	0.327	-6.37
8	*4*	*1.98*	*3.4*	*3His*	*2.99* *3.17* *4.19* *4.22*	*6.1* *6.1* *5.7* *5.7*	*122*	*0.309*	*-5.65*

[a] r is in units of Å; σ^2 is in units of 10^{-3} Å^2; ΔE_0 is in units of eV. All fits are to unfiltered EXAFS data over k = 1.5 – 13.0 Å^{-1}. In fits 5-8, the His imidazoles were treated as a rigid body, and included single scattering paths for Zn^{2+}–Cα and both three and four body paths involving Zn^{2+}– Cα–Cβ/Nβ (Cβ and Nβ are the more distant atoms of the imidazole). Fit 8 also included a three-body path for Zn^{2+}–N_{His}–Cα. The pathlengths for the rigid imidazole were constrained to a constant difference from one another and σ^2 was constrained to be identical for paths containing the same set of atoms.

Table S6. Selected unfiltered EXAFS fits to reconstituted ZnCA.[a]

	Zn-N/O			Zn•••C(His)					
fit	**n**	**r**	**σ^2**	**n**	**r**	**σ^2**	**F**	**F-factor**	**ΔE_0**
1	4	1.98	3.2				284	0.478	-5.70
2	5	1.98	4.6				295	0.486	-6.42
3	3 1	1.99 1.93	3.2 2.8				267	0.463	-5.44
4	4	1.98	3.1	6C	2.99	6.8	206	0.406	-6.21
5	***4***	***1.98***	***3.2***	***3His***	***2.99 4.19 4.21***	***7.0 6.0 6.0***	***115***	***0.303***	***-6.46***
6	4	1.97	3.1	4His	2.98 4.18 4.21	9.6 8.2 8.2	121	0.312	-7.00
7	4	1.98	3.2	2His	2.99 4.19 4.22	4.5 3.7 3.7	124	0.316	-6.28
8	4	1.97	3.1	3His	2.97 3.15 4.16 4.19	10.4 20.8 6.6 3.3	158	0.356	-6.40

[a] r is in units of Å; σ^2 is in units of 10^{-3} Å^2; ΔE_0 is in units of eV. All fits are to unfiltered EXAFS data over k = 1.5 – 13.0 Å^{-1}. In fits 5-8, the His imidazoles were treated as a rigid body, and included single scattering paths for Zn^{2+}–Cα and both three and four body paths involving Zn^{2+}– Cα–Cβ/Nβ (Cβ and Nβ are the more distant atoms of the imidazole). Fit 8 also included a three-body path for Zn^{2+}–N_{His}–Cα. The pathlengths for the rigid imidazole were constrained to a constant difference from one another and σ^2 was constrained to be identical for paths containing the same set of atoms.

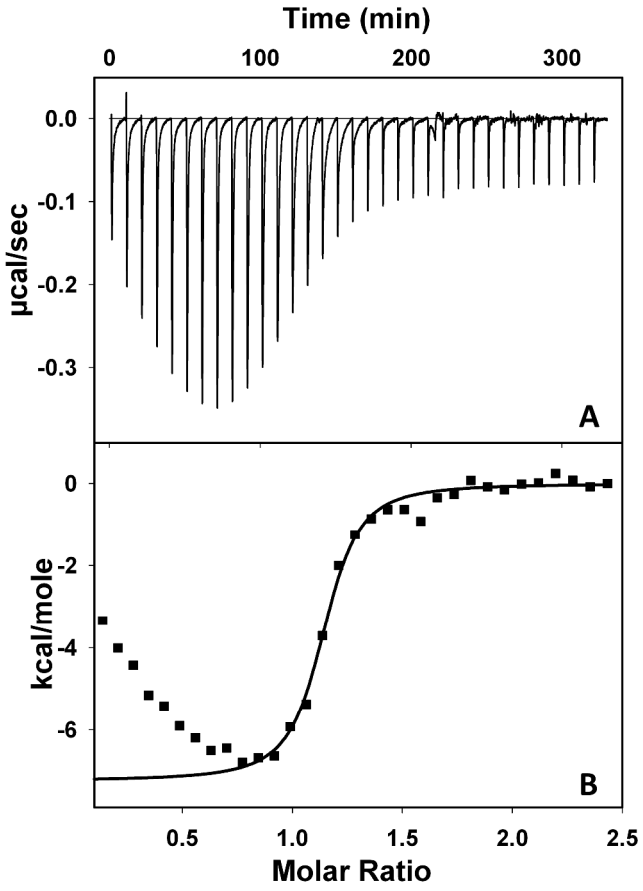

Figure S1. Reverse isothermal titration calorimetry data of apoCA binding to Zinc in PIPES buffer. (A) Raw data from the titration of a 1.5 mL cell containing 33 µM $Zn(NO_3)_2$ was titrated with 33 x 6 µL of 540 µM apoCA in 100 mM PIPES at pH 7.4. (B) Zn^{2+} binding isotherm and the best associated fit for a one-site binding model. n_{itc} = 1.1, K_{itc} = 5.0 × 10^6, ΔH_{itc} = -7.2 kcal/mol.

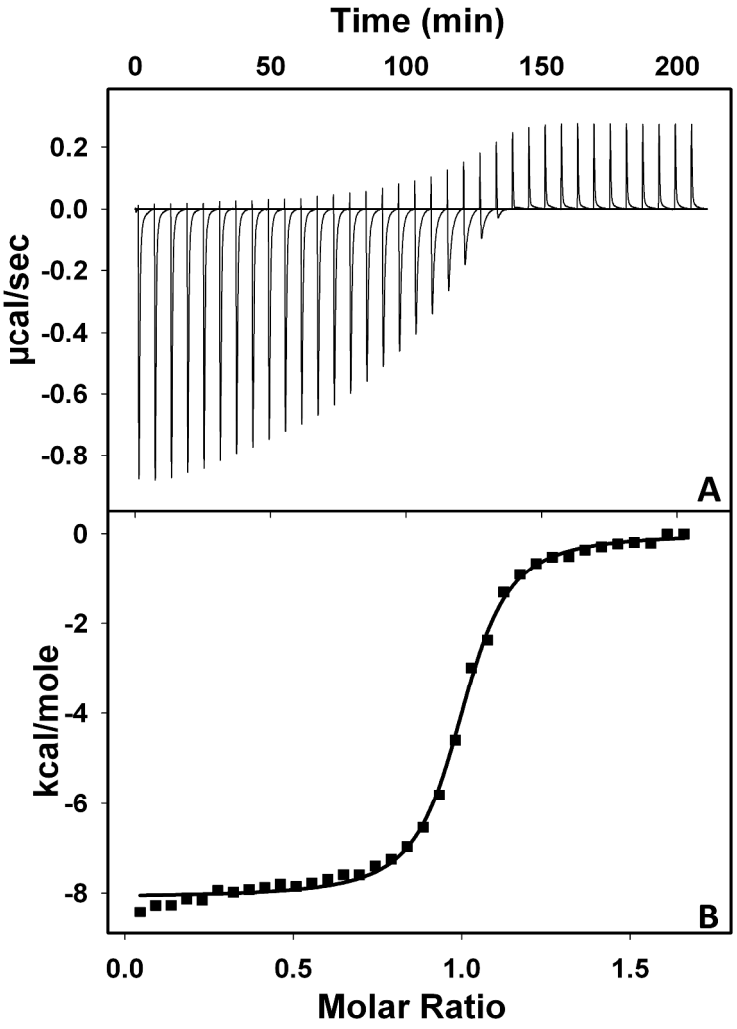

Figure S2. Isothermal titration calorimetry data of zinc binding to apoCA in MOPS buffer. (A) Raw data from the titration of a 1.5 mL cell containing 80 µM apo-CA was titrated with 35 x 3 µL of 1.85 mM $Zn(NO_3)_2$ in 100 mM MOPS at pH 7.4. (B) Integrated isotherm and the best associated fit for a one-site binding model. The average thermodynamic parameters associated with Zn^{2+} binding to apoCA are reported in Table 1.

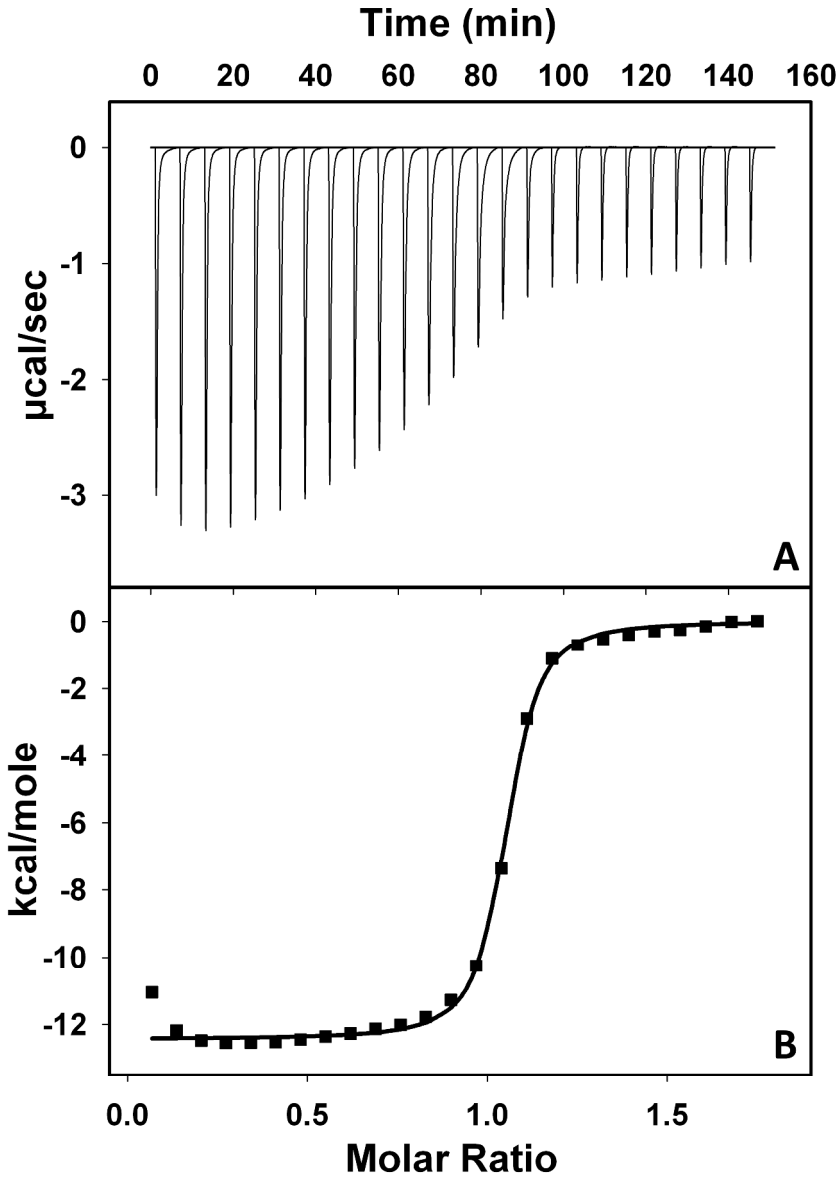

Figure S3. Isothermal titration calorimetry data of zinc binding to apoCA in Tris buffer. (A) Raw data from the titration of a 1.5 mL cell containing 70 µM apoCA was titrated with 25 x 3 µL of 2.26 mM $Zn(NO_3)_2$ in 100 mM Tris at pH 7.4. (B) Integrated isotherm and the best associated fit for a one-site binding model. The average thermodynamic parameters associated with Zn^{2+} binding to apoCA are reported in Table 1.

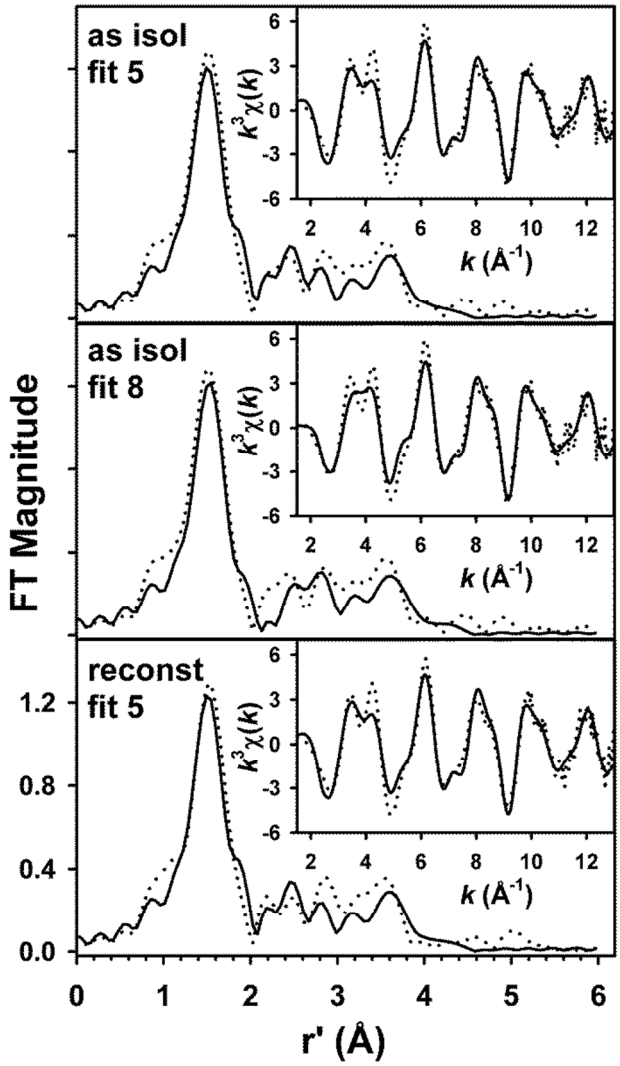

Figure S4. Comparison of the best fits given in the main manuscript (fit 5 for both as-isolated (top) and reconstituted (bottom) ZnCA, Tables S5 and S6, respectively) with another rigid imidazole fitting model that includes 3-body multiple scattering paths involving N_{His} and Cα of the His ligands (fit 8 for as-isolated ZnCA, middle plot and Table S5). Note the poorer match to the experimental $k^3\chi(k)$ EXAFS at $k \sim 4$ Å^{-1}, and subtle differences in the match to the Fourier transform.

Supplementary Remarks on the EXAFS Analysis

The results from EXAFS fitting of first-shell Fourier filtered $k^3\chi(k)$ EXAFS data for both as-isolated and reconstituted ZnCA are summarized in Table S4. In both cases, fits to 4 N/O scatterers at 1.98 Å provided the best match to experimental data, as judged by the goodness-of-fit metric *F'* and the bond valence sum value. Inclusion of a Zn–S interaction was not justified as the magnitude of ΔE_0 became unacceptably large (*c.f.* fits 12-13 for both samples, Table S4). This is in agreement with the measured XANES spectra, both of which lack the second intense peak after the white-line absorption that is associated with thiolate ligation in biological Zn(II) sites. Several attempts were made to split the primary shell into two subshells consisting of 3-4 Zn–N scatterers at 2.01 Å, presumably from bound His ligands, and 1 Zn–O scatterer at 1.85 – 1.90 Å that might reflect a bound water or hydroxide. The two shell fits produced a moderate improvement in fit quality relative to the simpler one-shell fits. However, the observed difference in refined absorber-scatterer distances for the two shells was generally smaller than the 0.14 Å resolution of the EXAFS data. We note that resolution in EXAFS is typically defined as $\pi/(2\bullet k_{range})$, where k_{range} is the range of the EXAFS data being fit in k space. In this case, the data was fit over k = 1.5-13.0 Å^{-1}, so k_{range} = 11.5 Å^{-1}. Therefore, the two shell fits cannot be justified, and the best fit to the first shell EXAFS data for both as-isolated and reconstituted ZnCA consists of 4 Zn–N/O scatterers at 1.98 Å (fit 2 for both samples, Table S4).

A similar sequence of best fits to the first coordination sphere was obtained in an analysis of the *unfiltered* $k^3\chi(k)$ EXAFS for as-isolated and reconstituted ZnCA (Tables S5 and S6, respectively). We were also able to treat outer-shell contributions from coordinated His ligands, with the following assumptions. The imidazole rings were treated as rigid bodies, with the Zn–N_{His}–C_2 and Zn–N_{His}–C_5 bond angles set to 125° and the displacement angle φ between the Zn–N bond axis and the plane of the imidazole ring set to ≤ 5°. During refinements, pathlengths associated with the His ligand (e.g. the two body Zn•••C_2/C_5 path and its three body counterpart Zn•••N_{His}•••C_2/C_5) were constrained to a constant difference from each other. Paths were grouped to represent an assumed average His position, as the specific contributions of each His imidazole cannot be deconvolved with any degree of accuracy. The inclusion of multiple-scattering paths from coordinated His ligands produced a substantial improvement in fit quality compared to simpler fits with only single-scattering paths (compare fit 4 with fit 5 in Tables S5 and S6). The best fit quality was obtained with 3 His ligands, although the fit quality differences with 2 His or 4 His were relatively subtle. Interestingly, fits in which the 3 body path Zn•••N_{His}•••C_2/C_5 was included gave somewhat poorer visual agreement with the experimental data, along with a decreased goodness-of-fit in the case of reconstituted ZnCA (compare fit 8 with fit 5 in Tables S5, S6 and Figure S4). While, it was not possible to perfectly reproduce the amplitudes of all features in the $k^3\chi(k)$ EXAFS or Fourier transforms, the spectral shapes were nicely reproduced by the constrained fitting model used in this analysis.

References

S1. Quinn, C. F. PhD thesis, **2009**, Dartmouth College

S2. Grossoehme, N. E.; Akilesh, S.; Guerinot, M. L.; Wilcox, D. E. *Inorg. Chem.* **2006**, *45*, 8500-8508.

S3. *NIST Standard Reference Database 46*, version 7.0; National Institute of Standards and Technology: Gaithersburg, MD, 2003.

S4. DiTusa, C. A.; Christensen, T.; McCall, K. A.; Fierke, C. A.; Toone, E. J. *Biochemistry* **2001**, *40*, 5338-5344.